THE JOURNAL OF BIOLOGICAL CHEMISTRY VOL. 286, NO. 37, pp. 32593–32605, September 16, 2011

LytN, a Murein Hydrolase in the Cross-wall Compartment of *Staphylococcus aureus*, Is Involved in Proper Bacterial Growth and Envelope Assembly*[S]

Received for publication, May 6, 2011, and in revised form, July 20, 2011 Published, JBC Papers in Press, July 22, 2011, DOI 10.1074/jbc.M111.258863

Matthew B. Frankel[1], **Antoni P. A. Hendrickx, Dominique M. Missiakas**[2], **and Olaf Schneewind**[2,3]

From the Department of Microbiology, University of Chicago, Chicago, Illinois 60637

Cell cycle progression for the spherical microbe *Staphylococcus aureus* requires the coordinated synthesis and remodeling of peptidoglycan. The majority of these rearrangements takes place at the mid-cell, in a compartment designated the cross-wall. Secreted polypeptides endowed with a YSIRK-G/S signal peptide are directly delivered to the cross-wall compartment. One such YSIRK-containing protein is the murein hydrolase LytN. *lytN* mutations precipitate structural damage to the cross-wall and interfere with staphylococcal growth. Overexpression of *lytN* also affects growth and triggers rupture of the cross-wall. The *lytN* phenotype can be reversed by the controlled expression of *lytN* but not by adding purified LytN to staphylococcal cultures. LytN harbors LysM and CHAP domains, the latter of which functions as both an *N*-acetylmuramoyl-L-alanine amidase and D-alanyl-glycine endopeptidase. Thus, LytN secretion into the cross-wall promotes peptidoglycan separation and completion of the staphylococcal cell cycle.

Staphylococcus aureus is a frequent cause of skin and soft tissue infections, sepsis, endocarditis, or pneumonia (1). Most antibiotics in current clinical use fail to treat infections with methicillin-resistant *S. aureus* (2); vancomycin and daptomycin are considered antibiotics of last resort for methicillin-resistant *S. aureus* infection; however, these compounds are also frequently associated with therapeutic failure (3, 4). The identification of new targets for antibiotic therapy and the development of new drugs for methicillin-resistant *S. aureus* infections are therefore urgently needed. *S. aureus* is a small spherical bacterium with a diameter of 800–1,000 nm and a surrounding thick layer of peptidoglycan cell wall (5). Staphylococcal cell wall synthesis begins in the cytoplasm where a sequence of reactions generates lipid II (C_{55}-PP-MurNAc(-L-Ala-D-iGlu-(NH_2-Gly_5)L-Lys-D-Ala-D-Ala)-GlcNAc). This product is translocated across the plasma membrane and polymerized into peptidoglycan strands with repeating disaccharide structure $(MurNAc\text{-}GlcNAc)_n$ (6–8). Neighboring peptidoglycan strands are cross-linked by penicillin-binding proteins (9), which form the amide bond between D-Ala at position four and the amino group of the pentaglycine (Gly_5) cross-bridge within the wall peptides of peptidoglycan strands (Fig. 1*A*) (10). The end product of the cell wall synthesis pathway, the murein sacculus, can be thought of as a large macromolecule that protects staphylococci from osmotic lysis (11). Peptidoglycan also serves as a scaffold for the anchoring and display of proteins, teichoic acids, and carbohydrates on the staphylococcal surface (12).

Shortly following cell division and separation, staphylococci assume a cell size that does not significantly increase prior to the next cell division (13, 14). Staphylococci synthesize a new layer of peptidoglycan at mid-cell in a compartment enclosed by membrane invaginations, which are formed following the constriction of FtsZ rings (5). This peptidoglycan synthesis compartment is designated the cross-wall (Fig. 1*B*). Once peptidoglycan synthesis in the cross-wall is completed, it separates two daughters that are half the size of the mother cell. Staphylococci cut the cross-wall peptidoglycan layer and separate their daughters (15). Because of high intracellular pressure, the former cross-wall section of each new daughter cell assumes the spherical shape of staphylococci. Daughter cells often remain connected through small segments of peptidoglycan. This pattern of incomplete cell wall separation produces the characteristic clusters of *S. aureus* cells (15). Incomplete separation of staphylococcal cells is exacerbated by mutations in either *atl* or *sle1*. Variants carrying deletions of *atl*, *sle1,* or both genes form abnormally large conglomerates of incompletely separated staphylococci, in agreement with the hypothesis that Atl and Sle1 contribute to the splitting of *S. aureus* cross-walls (16–18).

Atl is a prepro-protein. Following signal peptide removal, the pro-protein is cleaved, separating Atl amidase and glucosaminidase domains (19). Both domains possess repeat sequences that direct Atl enzymes to the vicinity of the cross-wall (19) (Fig. 1*C*). Sle1 is known to display *N*-acetylmuramoyl-L-Ala amidase activity (18). Unlike the Atl amidase, Sle1 harbors a cysteine, histidine-dependent amidohydrolase/peptidase (CHAP) domain (20, 21). Three LysM domains may be involved in directing Sle1 to the staphylococcal cell wall; however, the specific location of Sle1 within the staphylococcal cell wall envelope has not been revealed (18). Analyses of the genome sequence of *S. aureus* Newman identified four additional murein hydrolases, LytX (NWMN1667), LytY (NWMN2207), LytZ (NWMN2543), and LytN. LytX, LytY, and

* This work was supported, in whole or in part, by National Institutes of Health Grant AI038897 from Infectious Disease Branch, NIAID (to O. S.).

[S] The on-line version of this article (available at http://www.jbc.org) contains supplemental Figs. S1–S3.

[1] Supported by National Institutes of Health Postdoctoral Fellowship Award AI085709 from the NIAID.

[2] Member of and supported by the Region V "Great Lakes" Regional Center of Excellence in Biodefense and Emerging Infectious Diseases Consortium (recipient of NIAID Award 1-U54-AI-057153).

[3] To whom correspondence should be addressed: 920 E. 58th St., Chicago, IL 60637. Fax: 773-834-8150; E-mail: oschnee@bsd.uchicago.edu.

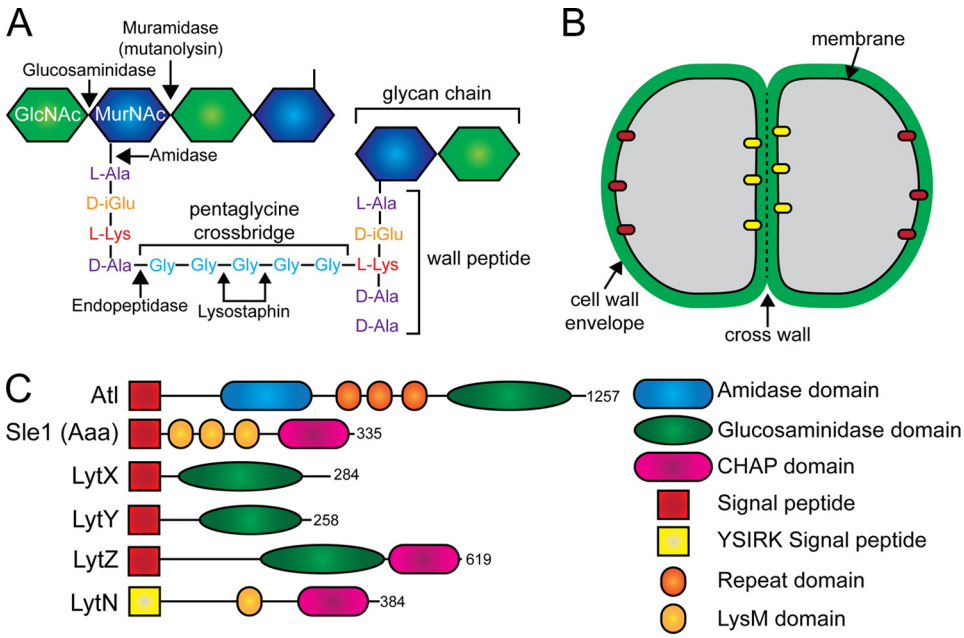

FIGURE 1. **Staphylococcal peptidoglycan and murein hydrolases.** *A*, illustration of staphylococcal peptidoglycan with selected enzymatic cleavage sites. *GlcNAc*, *N*-acetylglucosamine; *MurNAc*, *N*-acetylmuramic acid. *B*, schematic of a dividing staphylococci illustrating the location of the cell wall envelope, membrane, and cross-wall. *Yellow* and *red ovals* represent translocons for the secretion of YSIRK/GS (*yellow*) and conventional signal peptide precursors (*red*), respectively. *C*, diagram of chromosomally encoded murein hydrolases with N-terminal signal peptides of *S. aureus* strain Newman. Functional domains predicted to exert specific hydrolytic activities are listed.

LytZ all possess an N-terminal signal peptide and glycosaminidase domain, with LytZ also containing a CHAP domain (Fig. 1*C*) (22). Other murein hydrolases lack signal peptides and likely require bacteriophage holins for export from the cytoplasm (23). All *S. aureus* isolates sequenced to date encode the *lytN* gene whose translational product is endowed with a YSIRK/GS-type signal peptide, CHAP and LysM domains. Precursor proteins with YSIRK/GS-type signal peptides are secreted into the cross-wall of *S. aureus* (24). Most of these proteins carry C-terminal sorting signals and, following cleavage by sortase A, are covalently linked to pentaglycine crossbridges in the cross-wall (25, 26). The *lytN* gene was first described as being located immediately adjacent to *fmhC*, a homolog of *femA*, whose translational product transfers glycyl residues from glycyl-tRNA to the ϵ-amino group of L-Lys within lipid II (7, 27, 28). The contribution of *lytN* to staphylococcal growth and cell wall synthesis or degradation was previously not studied. In this study, we report that disruption of *lytN* results in a retardation of growth, gross abnormalities to the cell wall, in particular the cross-wall of dividing staphylococci, and biochemically characterizes the muralytic properties of LytN.

EXPERIMENTAL PROCEDURES

Bacterial Strains and Reagents—*S. aureus* Newman (22) and its variant carrying a bursa aurealis insertion in *lytN* are part of the Phoenix library (29). The *lytN* mutational lesion was transduced with bacteriophage ϕ85 into the wild-type *S. aureus* Newman isolate (30). Plasmid DNA was first electroporated into *S. aureus* RN4220 (31) and then into the *S. aureus* Newman or the *lytN* mutant strain. *S. aureus* was grown in tryptic soy broth or on tryptic soy agar plates supplemented with appropriate antibiotics. Erythromycin and chloramphenicol were used at a concentration of 10 μg/ml. *Escherichia coli* was grown in LB broth or on LB agar plates supplemented with either ampicillin (100 μg/ml) or kanamycin (50 μg/ml). All chemicals used were purchased from either Sigma or Fisher, unless otherwise stated. Lysostaphin was purchased from AMBI Products.

lytN Expression Vectors and Protein Purification—For inducible expression of *lytN* in staphylococci, primers 5′-ggCCTAGGAGGAGGacagctatgtttttatattattgtaaggagtgtttcatc-3′ and 5′-gatcCCGCGGttatgctttttttaaatggtctaataaaaatc-3′ were used, which incorporate AvrII and SacII restriction sites, respectively, and permit amplification of *lytN* using *S. aureus* Newman genomic DNA as template. The PCR products, along with pMF312 (harboring the anhydrotetracycline-inducible promoter, iTet, on a replicating plasmid) (32), were digested with AvrII/SacII and ligated. Plasmid DNA was sequenced to confirm an error-free construct and introduced into *S. aureus* RN4220, followed by electroporation into wild-type *S. aureus* Newman or the isogenic *lytN* mutant.

A LytN-mCherry construct for expression in *S. aureus* was generated by SOE[4] PCR. *lytN* was amplified using 5′-ggCCTAGGaggaggacagctatgtttttatattattgtaaggagtgtttcatc-3′ and 5′-ctcgcccttgcttgctttttttaaatggtctaataaaaatcat-3′, whereas *mCherry* was amplified using 5′-tttaaaaaagcaagcaagggcgaggaggataacatgg-3′ and 5′-gatcCCGCGGttacttgtacagctcgtccatgcc-3′. Underlined sequence denotes complementary sequence for the SOE reaction. Uppercase sequence indicates AvrII and SacII restriction sites, respectively. The two PCR products were isolated using the Qiaquick PCR cleanup kit (Qiagen) and combined for the SOE reaction using the 5′ primer of *lytN* and the 3′ primer

[4] The abbreviations used are: SOE, splicing by overlap extension; rpHPLC, reversed-phase HPLC; PT, phenylthiohydantoin; rLytN, recombinant LytN.

of *mCherry*. The PCR product and pCL55itet (33, 34) were cut with AvrII and SacII and ligated as described above.

For expression and purification of recombinant LytN (rLytN), the signal peptide-less gene was amplified using primers 5′-ccGGATCCGgatgaaattgataaatctaaagattttacaagag-3′ and 5′-ggCTCGAGtgctttttttaaatggtctaataaaaatcat-3′, incorporating BamHI and XhoI sites, respectively. The PCR product, along with the pET24b vector, were cut with the corresponding enzymes and ligated, generating a C-terminal six histidyl tag for affinity chromatography. Plasmid prLytN was analyzed by DNA sequencing and transformed into *E. coli* BL21 (DE3).

To generate a C-terminal mCherry hybrid to LytN, SOE PCR was used and cloned as described above using primers 5′-ccGGATCCGgatgaaattgataaatctaaagattttacaagag-3′ and 5′-ctcgccttgcttgctttttttaaatggtctaataaaaatcat (for *lytN*), and 5′-tttaaaaaagcaagcaagggcgaggaggataacatgg-3′ and 5′-ggCTCGAGcttgtacagctcgtccatgcc-3′ (*mCherry*). The SOE reaction product was ligated into pET24b using BamHI and XhoI restriction sites. Truncation of the CHAP domain was performed using the primers 5′-ccGGATCCGgatgaaattgataaatctaaagattttacaagag-3′ and 5′-ggCTCGAGactattacttttattatttgaagacactgttttg-3′ and cloned as described above. LytN amino acid substitutions were performed by QuikChange mutagenesis (Stratagene) using primers 5′-ggtagttatggatggcaaGCTttcgatttagttaatgta-3′ and 5′-tacattaactaaatcgaaAGCttgccatccataactacc-3′ for the C266A mutation or 5′-tttggtggaggatatggtGCTacagctattgtcttaaat-3′ and 5′-atttaagacaatagctgtAGCaccatatcctccaccaaa-3′ for the H329A mutation. prLytN was used as template for mutagenesis.

To purify rLytN, *E. coli* BL21 (DE3, prLytN) was grown to an A_{600} 0.6 and rLytN, expression was induced with 1 mM isopropyl 1-thio-β-D-galactopyranoside for 4 h at 37 °C. Cells were sedimented by centrifugation, suspended in column buffer (50 mM NaH_2PO_4, 300 mM NaCl, 10 mM imidazole, pH 8.0), and lysed by two passages in a French pressure cell (14,000 pounds/inch^2). Lysates were cleared by centrifugation at 30,000 × *g* and subjected to affinity chromatography on nickel-nitrilotriacetic acid-Sepharose. The column was washed with column buffer containing 10 or 20 mM imidazole. rLytN was eluted in column buffer with 250 mM imidazole and dialyzed against column buffer without imidazole.

Purification and Digestion of Peptidoglycan—Peptidoglycan purification was performed as described previously (35). Briefly, 2 liters of staphylococci were grown to an A_{600} 0.6, quickly cooled to 4 °C in an ice bath, and centrifuged. Cells were washed in water, suspended in 4% SDS, and boiled for 30 min. Detergent was removed by washing cells extensively in water. Staphylococci were subjected to bead beating, and glass beads were removed, and cell debris was sedimented by centrifugation. The extract was incubated with amylase for 2 h, followed by the addition of DNase and RNase for 2 h, and finally trypsin was added and incubated for 16 h at 37 °C. Peptidoglycan extracts were centrifuged, washed with water, and suspended in 1% SDS and boiled for 15 min to heat-inactivate all enzymes. Peptidoglycan was extensively washed with water to remove all traces of SDS, followed by washing with 8 M LiCl, 100 mM EDTA, and acetone. Cell walls were then washed with water and lyophilized. Hydrofluoric acid was then added and incubated for 48 h at 4 °C to remove teichoic acid. Peptidoglycan was neutralized, and the pellet was treated with alkaline phosphatase for 16 h at 37 °C. Purified peptidoglycan was boiled for 5 min, washed with water, and stored at 4 °C.

Peptidoglycan, adjusted for concentration by A_{600}, was incubated for 16 h at 37 °C with 100 μl of enzyme:lysostaphin (2 mg/ml), mutanolysin (7,000 units/ml), or rLytN (300 μg/ml). Peptidoglycan samples were incubated in 12.5 mM phosphate buffer, pH 5.5 (mutanolysin), 50 mM phosphate buffer, pH 5.5 (rLytN), or 50 mM Tris-HCl, pH 7.5, 150 mM NaCl (lysostaphin). After 16 h of incubation, peptidoglycan samples were boiled for 10 min and centrifuged at 15,000 × *g* for 15 min. Soluble material was either incubated with rLytN or reduced via the addition of 0.5 M sodium borate and 3–5 mg of sodium borohydride. Samples were incubated for 30 min and inactivated by the addition of 20% phosphoric acid to reach pH <4.0.

Purification of Muropeptides and Mass Spectrometry—Reduced muropeptides were separated by rpHPLC on 250 × 4.6-mm ODS hypersil C18 column (Thermo Scientific). Individual peaks were desalted as described previously (36). Desalted muropeptides were dried under vacuum, suspended in 5–30 μl of 30% acetonitrile, and 0.5 μl were co-spotted with 0.5 μl of matrix, α-cyano-4-hydroxycinnamic acid, at 10 mg/ml in 50% acetonitrile, 0.1% trifluoroacetic acid (TFA). Samples were subjected to MALDI-TOF mass spectrometry using a Autoflex Speed Bruker MALDI instrument. Ions were detected in reflectron positive mode. For Edman degradation, purified muropeptides were desalted by rpHPLC, dried under vacuum, and analyzed by a Procise 494 HT sequencer (PerkinElmer Life Sciences and University of Illinois at Urbana-Champaign Protein Sciences Facility).

Immunoblotting and Microscopy—Staphylococci were grown to mid log phase, sedimented by centrifugation, and incubated with mutanolysin, lysostaphin, or rLytN. Proteins were precipitated with 7.5% trichloroacetic acid and washed with ice-cold acetone. Protein samples were dried, solubilized in sample buffer, and separated on 10% SDS-PAGE. Following electro-transfer to PVDF membrane (Millipore), residual binding sites on the filter were blocked with 5% milk in PBS, 0.1% Tween 20. For SpA detection, monoclonal antibodies (SPA-27; Sigma) were used. Secondary antibodies were HRP-conjugated (Cell Signaling Technology) and visualized following incubation with ECL solution.

Fluorescent microscopy was performed by first fixing cells in 2.5% paraformaldehyde, 0.006% glutaraldehyde, 30 mM $NaPO_4$, pH 7.4, for 20 min. Cells were blocked in PBS containing 3% BSA and stained with BODIPY-vancomycin as described previously (37). Cells were applied to polylysine-treated glass coverslips and mounted onto glass slides containing a drop of SlowFade anti-fading reagent (Invitrogen). Images were captured on a Leica TCS SP2 AOBS laser scanning confocal microscope with 100× oil objective.

Electron Microscopy—Transmission electron microscopy was performed essentially as described previously (34). For scanning electron microscopy, staphylococci were suspended in H_2O, washed twice, fixed for 30 min in 2% glutaraldehyde in phosphate-buffered saline (PBS) at room temperature, and post-fixed for 30 min in glutaraldehyde onto freshly prepared

poly-L-lysine-coated glass coverslips. Samples were washed twice with PBS and subsequently serially dehydrated by consecutive incubations in 25 and 50% ethanol/PBS, 75 and 90% ethanol/H_2O, 2× 100% ethanol, followed by 50% ethanol/hexamethyldisilazane and finally with 100% hexamethyldisilazane. After overnight evaporation of hexamethyldisilazane at room temperature, samples were mounted onto specimen mounts (Ted Pella, Inc., Redding, CA) and coated with 80% platinum, 20% palladium to 8 nm using a Cressington 208HR Sputter Coater at 20 mA prior to examination with a Fei Nova NanoSEM 200 scanning electron microscope (FEI Co., Hillsboro, OR). The S.E. was operated with an acceleration voltage of 5 kV, and samples were viewed at a distance of 5 mm (38).

Circular Dichroism—Recombinant proteins were purified as described above and dialyzed against 10 mM sodium phosphate buffer, pH 6.0, 50 mM sodium sulfate. Proteins were then analyzed with a AVIV 202 CD Spectrometer in the far-UV range. Readings were taken in triplicate, buffer subtracted, and plotted.

RESULTS

lytN Is Required for Proper Staphylococcal Growth—The *lytN* open reading frame is composed of 384 codons (22). A bursa aurealis insertion at codon 258 of *lytN* from the Phoenix library (29) was transduced with bacteriophage ϕ85 into the wild-type strain *S. aureus* Newman. The mutational lesion was verified by DNA sequencing. Wild-type and *lytN* strains were cultured in tryptic soy broth at 37 °C, and growth was monitored as an increase in absorbance (A_{600}). Compared with *S. aureus* Newman, the *lytN* mutant multiplied more slowly and, during stationary phase, failed to reach the same density (Fig. 2). We also measured staphylococcal growth by plating culture aliquots on agar media followed by enumeration of colony-forming units; the *lytN* mutant displayed a similar growth defect in this assay (data not shown). The *lytN* growth defect was restored to wild-type levels when a copy of the intact *lytN* gene was supplied on a plasmid under the control of the anhydrotetracycline-inducible promoter (Fig. 2). Expression of *lytN* in the resulting strain, *lytN* (P_{tet}::*lytN*), can be induced with anhydrotetracycline, although the regulation of expression is incomplete (34). The phenotype of *lytN* mutants was restored to wild-type levels by growth of *lytN* (P_{tet}::*lytN*) staphylococci in the absence of the anhydrotetracycline inducer (Fig. 2).

Staphylococci were grown to mid-logarithmic phase, fixed, embedded in paraffin, thin-sectioned, stained with uranyl acetate, and examined for their cell wall envelope structure by transmission electron microscopy. As expected, *S. aureus* Newman elaborated murein sacculi and cross-walls with characteristic thickness and uniform integrity (5). In contrast, the cell wall envelope of *lytN* mutants appeared irregular in structure with discrete layers of peptidoglycan that were disintegrated and distorted in their spherical shape (Fig. 2). Scanning electron microscopy experiments corroborated these findings. Images of wild-type staphylococci revealed the characteristic round cell shape with equatorial surface rings, the binding sites for the cell separation enzyme Atl. In contrast, the surface of *lytN* mutants appeared irregular, and the spherical shape of mutant cells appeared deformed. Cell division sites and equatorial sur-

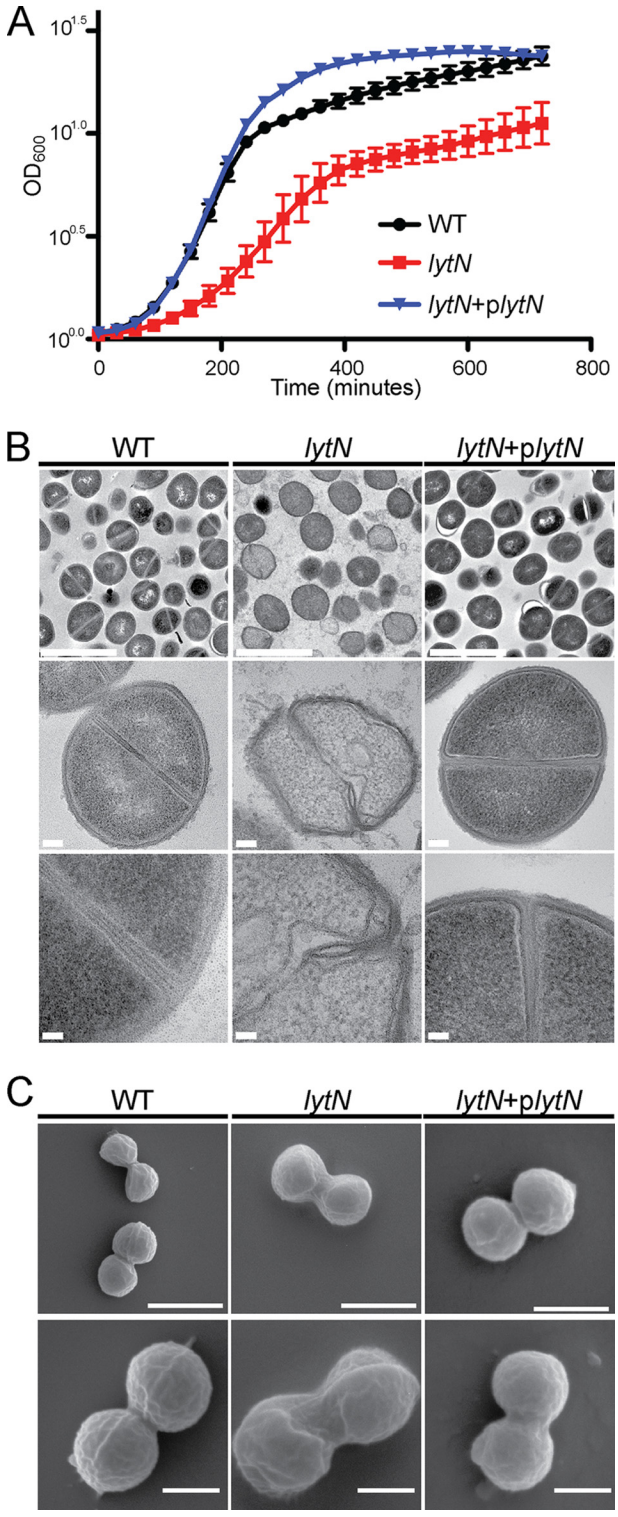

FIGURE 2. ***lytN* mutation results in *S. aureus* growth defects and altered cellular morphology.** *A*, growth rate of wild-type *S. aureus* Newman, its *lytN* variant, and the complemented mutant was interrogated by monitoring the absorbance at A_{600} over 12 h at 37 °C. Experiments were performed in triplicate, and *error bars* represent the means ± S.E. *B*, transmission electron micrograph of wild-type (*WT*), *lytN* mutant, and the *lytN* complemented cells grown to mid-logarithmic phase. *Scale bar* for *top panels* is 2 μm; *middle panels* is 100 nm; *bottom panels* is 50 nm. *C*, scanning electron micrographs of WT, *lytN*, and the *lytN* complemented mutant cells as described above. *Scale bar* for *top panels* is 1 μm, and *bottom panels* is 500 nm.

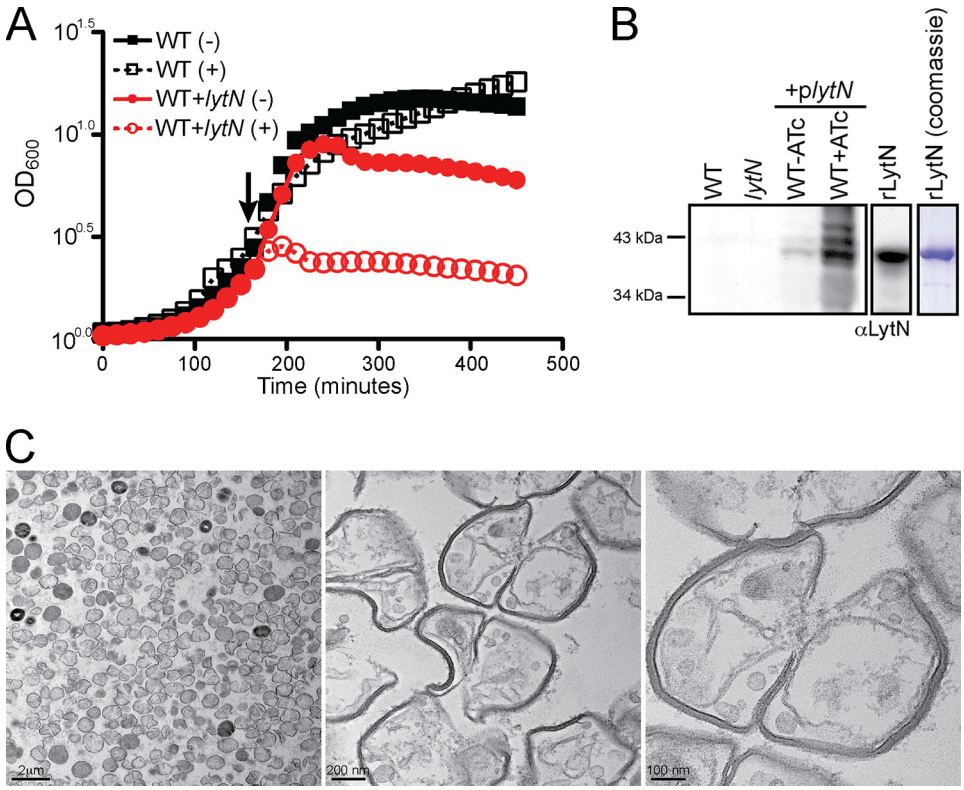

FIGURE 3. **Overexpression of *lytN* causes cellular lysis at the cross-wall.** *A*, wild-type staphylococci with or without a multicopy vector expressing *lytN* under the control of the anhydrotetracycline-inducible promoter were grown for 2.5 h at 37 °C. At this point, inducer was added to cells, and absorbance at A_{600} was monitored for growth over time. Experiments were performed in triplicate, and *error bars* represent the means ± S.E. *B*, immunoblot analysis of *lytN* production using specific rabbit antisera. Wild-type, *lytN* mutant, and wild-type containing p*lytN* were grown as described above, and total proteins were harvested. rLytN was loaded alongside staphylococcal lysates as a control, and samples were either examined by immunoblot or stained with Coomassie Brilliant Blue. *C*, transmission electron micrographs of wild-type staphylococci induced for overexpression of *lytN* for 30 min. Cells were fixed, thin-sectioned, and negatively stained prior to electron microscopic examination.

face rings could not be clearly discerned in images of *lytN* mutant cells. Moreover, daughter cell separation appeared impaired, implying a role for LytN in cell separation. Introduction of the wild-type *lytN* gene in *trans* restored the structural features of peptidoglycan in the cell wall envelope and cross-wall of *lytN* mutants to those observed in wild-type staphylococci (Fig. 2).

Overexpression of lytN Triggers Lysis of the Staphylococcal Cross-wall—Anhydrotetracycline induction of P_{tet}::*lytN* in the strain *lytN* (P_{tet}::*lytN*) inhibited bacterial growth (data not shown). We generated a variant of wild-type *S. aureus* Newman carrying a multicopy plasmid harboring *lytN*, again under the control of anhydrotetracycline (wild-type (P_{tet}::*lytN*)). In the absence of the anhydrotetracycline inducer, wild-type (P_{tet}::*lytN*) staphylococci grew during exponential phase but failed to reach the same density as the wild-type parent (Fig. 3). This is due to the incomplete suppression of expression in this multicopy vector (Fig 3*B*). In the presence of the inducer, wild-type (P_{tet}::*lytN*) cells ceased growth and declined in absorbance (A_{600}) (Fig. 3). To assess whether growth inhibition was caused by the increased expression of *lytN*, extracts derived from wild-type staphylococci, *lytN* and wild-type strains harboring (P_{tet}::*lytN*), were subjected to immunoblotting experiments using LytN-specific rabbit antisera (Fig. 3). LytN was detected in wild-type strains harboring (P_{tet}::*lytN*), but not in the wild-type parent or *lytN* mutant staphylococci lacking inducible expression of *lytN*. The overall abundance of LytN was increased in wild-type (P_{tet}::*lytN*) cells that had been grown in the presence of the inducer (Fig. 3). Wild-type (P_{tet}::*lytN*) staphylococci incubated in the presence of anhydrotetracycline were fixed and thin-sectioned, and uranyl acetate stained samples were viewed by transmission electron microscopy. These images revealed that the cell wall envelope of P_{tet}::*lytN* staphylococci was largely intact but the cross-wall peptidoglycan had in part disintegrated. Almost all staphylococci in these samples were lysed, and the sites of their rupture were located in the cross-wall compartment. In sum, we presume physiological levels of *lytN* expression are low, as the enzyme could not be detected with LytN-specific antibodies. Growth defect and structural damage to the cross-wall of *lytN* mutants could be complemented with P_{tet}::*lytN*. Overexpression of *lytN* triggered rupture of the cross-wall and staphylococcal lysis.

Localization of LytN in the Staphylococcal Envelope—Anhydrotetracycline-induced expression of the translational hybrid *lytN-mCherry* resulted in lysis of wild-type cells (P_{tet}::*lytN-mCherry*) (data not shown), indicating that LytN-mCherry is functionally active. To circumvent this issue and to more carefully control the expression of *lytN*-mCherry, the translational hybrid was expressed from the integrative vector, pCL55iTET, again under the control of anhydrotetracycline but allowing a more tight regulation (Refs. 32, 33 and data not shown). BODIPY-vancomycin, which binds to the terminal

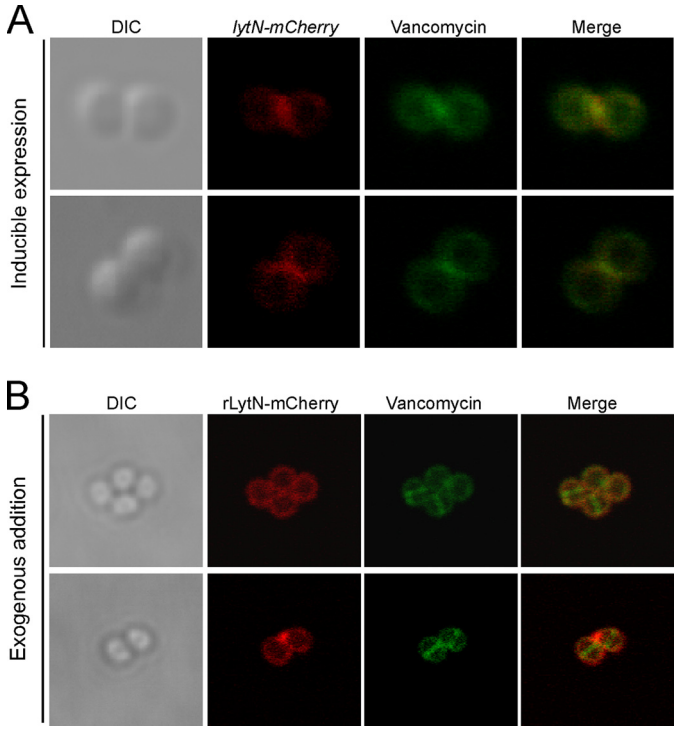

FIGURE 4. **LytN is directly trafficked to the cross-wall.** *A,* wild-type *S. aureus* encoding *lytN-mCherry* under the control of an anhydrotetracycline-inducible promoter from an integrative vector was grown to mid-logarithmic phase, and inducer was briefly added. Shortly thereafter, cells were fixed and stained with BODIPY-vancomycin. Micrographs are arranged in the following order from *left to right*: differential interference contrast (*DIC*), mCherry fluorescence, BODIPY-vancomycin fluorescence, and the merged fluorescent images. Two representative images are presented. *B,* recombinant LytN-mCherry was added to staphylococci and allowed to bind for 15 min, and samples were washed with PBS, fixed with paraformaldehyde, and stained with BODIPY-vancomycin. Images were acquired as described in *A*.

D-Ala within the wall peptide of peptidoglycan, was used to visualize the staphylococcal cell wall envelope and its cross-wall in fluorescence microscopy experiments (37). Upon brief anhydrotetracycline induction of P_{tet}::*lytN-mCherry* cells, red fluorescent staining initially appeared near the cross-wall and the BODIPY-vancomycin fluorescent compartment between adjacent daughter cells (Fig. 4*A*). Over time, LytN-mCherry appeared throughout the cell wall as peptidoglycan synthesis and cell division continued, resulting in cell lysis (data not shown). rLytN-mCherry was purified from recombinant *E. coli* and added to staphylococcal cells. Cells were washed, stained with BODIPY-vancomycin, and viewed by fluorescence microscopy. Red fluorescence staining was observed throughout the cell wall envelope with some accumulation in cell wall envelope sections that surround the perpendicular cross-wall (Fig. 4*B*). Of note, red fluorescence signals were not detected in the staphylococcal cross-wall, despite BODIPY-vancomycin staining at this site (Fig. 4*B*). These data suggest that vancomycin, but not exogenously added polypeptides (rLytN-mCherry), penetrate the cross-wall of staphylococci. Conversely, the LytN-mCherry precursor, which is endowed with a YSIRK/GS signal peptide, appears to be secreted into the cross-wall compartment.

Purified rLytN Cleaves Staphylococcal Peptidoglycan—Purified rLytN was added to staphylococcal cultures, and growth

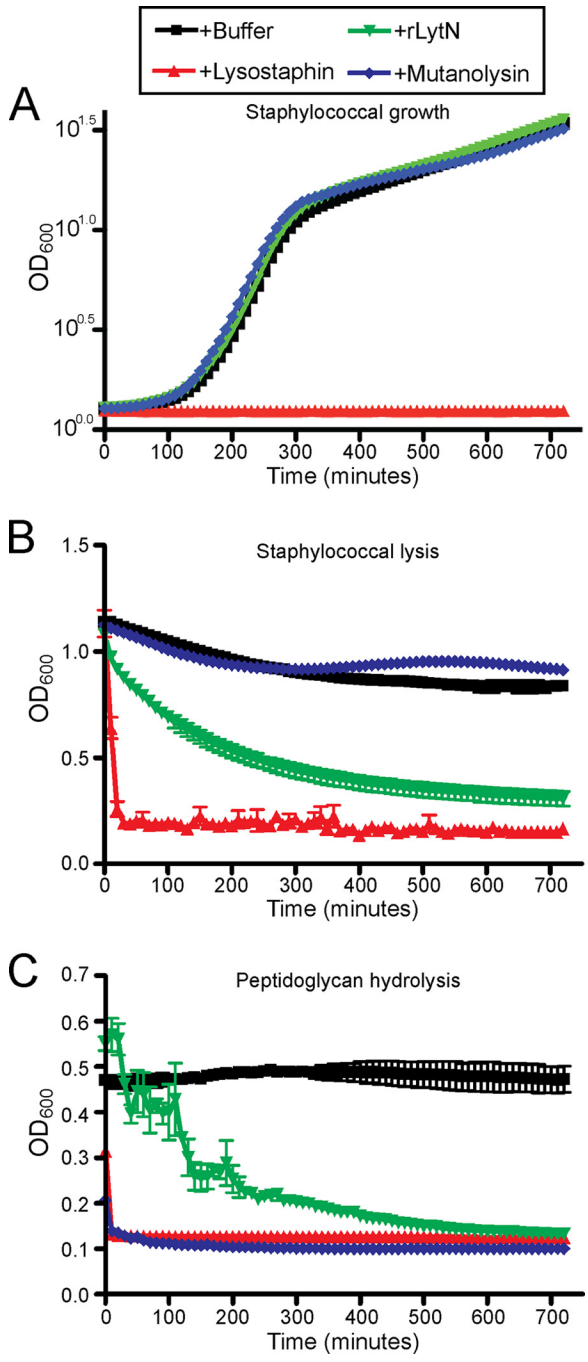

FIGURE 5. **Comparison of rLytN with other murein hydrolases.** *A,* an overnight culture of *S. aureus* Newman was diluted into fresh media supplemented with buffer, lysostaphin, mutanolysin, or recombinant LytN (rLytN), and growth was monitored over 12 h at 37 °C by A_{600} readings. Conditions were performed in triplicate, and *error bars* represent the means ± S.E. *B,* staphylococci grown to stationary phase were washed in buffer and subsequently incubated in the presence of buffer alone, lysostaphin, mutanolysin, or rLytN. Cell lysis was monitored by A_{600} over time as in *A*. *C,* purified staphylococcal peptidoglycan was incubated with buffer alone, lysostaphin, mutanolysin, or rLytN, and hydrolysis was measured by monitoring A_{600} over 12 h.

was monitored as an increase in absorbance at 600 nm light (A_{600}). As controls, lysostaphin, the staphylolytic glycyl-glycine endopeptidase (39), prevented bacterial growth, whereas mutanolysin, a streptomycetal muramidase (40), did not (Fig. 5*A*). Purified rLytN also did not interfere with staphylococcal

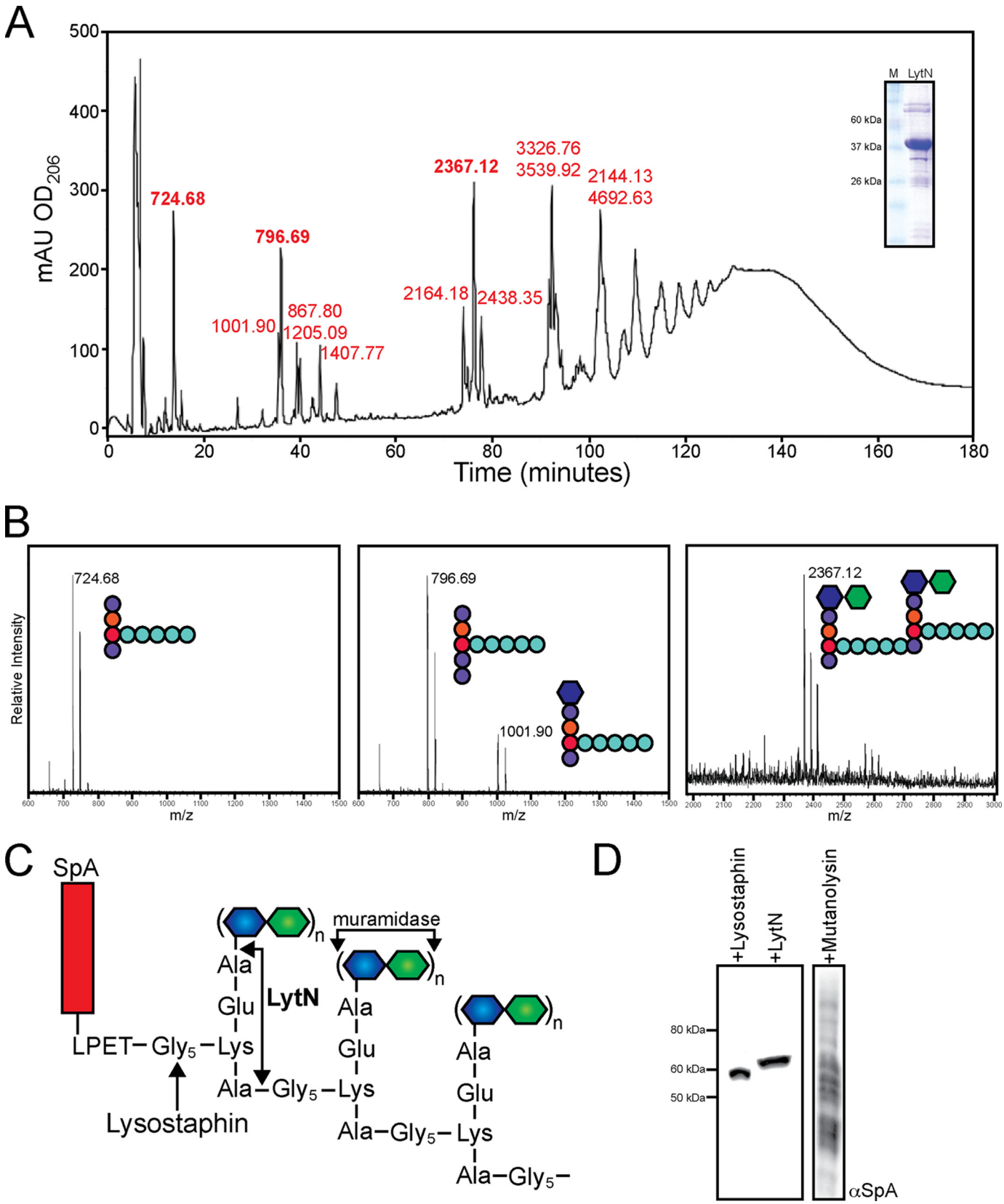

FIGURE 6. **rLytN functions as an amidase and endopeptidase.** *A*, *S. aureus* wild-type peptidoglycan was treated with recombinant LytN for 16 h at 37 °C, reduced, and resolved by rpHPLC as described under "Experimental Procedures." Individual peaks were desalted and subjected to MALDI-TOF MS, with observed *m/z* listed in *red above* each peak tested. *Inset*, Coomassie-Brilliant Blue-stained SDS-PAGE of rLytN. *B*, example mass spectra obtained from the three most prominent peaks shown in *A* (*m/z* 724.68, 796.69, and 2367.12), with the proposed structure for each compound (see Fig. 1 for color coding). *C*, diagram of cell wall anchored protein A (*SpA*). The cleavage sites of lysostaphin, mutanolysin, and LytN are noted with *arrows*. *D*, immunoblot with SpA-specific monoclonal antibody from protein lysates derived from staphylococci treated with lysostaphin, rLytN, or mutanolysin. *mAU*, milliabsorbance units.

TABLE 1
MALDI-TOF MS of rLytN-released peptidoglycan fragments
See Fig. 7*A* for absorption peaks of rpHPLC of rLytN-treated *S. aureus* peptidoglycan. Observed and calculated *m/z* values are for sodiated ions.

Compound	*m/z*		Δ (observed and calculated)	Predicted structure
	Observed	Calculated		
1	724.68	724.72	−0.04	$AQKG_5A$
2	796.69	795.80	0.89	$AQKG_5AA$
3	867.80	867.41	−0.039	$AQKG_5A_3$
4	1001.90	1001.01	0.89	MurNAc-$AQKG_5A$
5	1205.09	1205.20	0.11	GlcNAc-MurNAc-$AQKG_5A$
6	1407.77	1407.27	−0.41	$GlcNAc_2$-MurNAc-$AQKG_5A$
7	2164.18	2163.92	−0.26	GlcNAc-$MurNAc_2$-$(AQKG_5A)_2$
8	2367.12	2367.38	−0.026	$(GlcNAc\text{-}MurNAc)_2$-$(AQKG_5A)_2$
9	2438.35	2438.03	−0.32	$(GlcNAc\text{-}MurNAc)_2$-$(AQKG_5A)_3$

growth (Fig. 5*A*). Incubation of stationary phase *S. aureus* cells with chaotropic agents or murein hydrolases may cause staphylococcal lysis, detected as a decline in A_{600}. Addition of lysostaphin to stationary phase staphylococci triggered rapid lysis, whereas mutanolysin had no effect (Fig. 5*B*). The addition of rLytN to stationary phase cultures caused partial staphylococcal lysis (Fig. 5*B*). Peptidoglycan of *S. aureus* was isolated and degraded with either lysostaphin or mutanolysin, which was measured as a decline in A_{600} (Fig. 5*C*). rLytN also displayed peptidoglycan hydrolase activity (Fig. 5*C*). Compared with similar amounts of lysostaphin or mutanolysin, rLytN degraded less peptidoglycan. Taken together, these data indicate that rLytN, which does not display autolysin activity, functions as a murein hydrolase that cleaves *S. aureus* peptidoglycan.

Muropeptide Profile of Wild-type and lytN Mutant Staphylococci—We wondered whether *lytN* mutants harbor changes in peptidoglycan structure when compared with wild-type staphylococci. Murein sacculi of *S. aureus* Newman and the isogenic *lytN* mutant were isolated, and peptidoglycan was purified. The peptidoglycan was treated with mutanolysin, which cleaves the glycosidic bond between MurNAc-(β1–4)-GlcNAc, releasing disaccharide muropeptides that were reduced with sodium borohydride and separated by rpHPLC. As expected, muramidase treatment of wild-type peptidoglycan released disaccharide tetrapeptide, disaccharide pentapeptide, and tetrasaccharide peptidoglycan fragments (supplemental Fig. S1). Similar results were observed when the cell wall of the *lytN* mutant was cleaved with muramidase, indicating that the overall structure of peptidoglycan is not altered by the insertional disruption of the *lytN* gene (supplemental Fig. S1).

Characterization of Peptidoglycan Fragments Released with rLytN—Purified peptidoglycan of wild-type staphylococci was treated with rLytN, and soluble fragments were subjected to rpHPLC (Fig. 6*A*). Isolated compounds were dried, again subjected to rpHPLC for salt removal, and analyzed by matrix-assisted laser desorption ionization time of flight (MALDI-TOF) mass spectrometry. Ion signals at *m/z* 724.68 (13 min) and 796.69 (35 min) were explained as the sodium ions of NH_2-L-Ala-iGln-L-Lys-(NH_2-Gly_5)-D-Ala-COOH (calculated mass of 724.72) and NH_2-L-Ala-iGln-L-Lys-(NH_2-Gly_5)-D-Ala-D-Ala-COOH (calculated mass 795.80). The ion at *m/z* of 2367.12 (75 min) corresponded to the cross-linked disaccharide peptidoglycan fragment MurNAc-(L-Ala-iGln-L-Lys-(NH_2-Gly_5)-D-Ala-COOH)-(β1–4)-GlcNAc (calculated mass 2367.38) (Fig. 6*B*). A complete list of peptidoglycan fragments with their observed mass and predicted structure is provided in Table 1. To confirm the identity of sodiated ions, CsCl (cesium *m/z* 132.90) was added to samples. The addition of cesium can displace sodium ions (*m/z* 22.99) and should consequently increase the mass to charge ratio by *m/z* 110. Indeed, we observed increases in *m/z* 110 for the sodium ions of rLytN-released peptidoglycan fragments (supplemental Fig. S2). Together, these data suggest that rLytN cleaves the staphylococcal peptidoglycan at two positions, the amide bonds between MurNAc and L-Ala as well as D-Ala-Gly. If so, Edman degradation of peptidoglycan fragments should release phenylthiohydantoin-Ala (PT-Ala) and phenylthiohydantoin-Gly (PT-Gly), respectively. This was tested, and compounds with *m/z* 724.68 and 796.69 released equimolar amounts of PT-Ala and PT-Gly after the first cleavage cycle, followed by four cycles of PT-Gly release (the amide bond between D-iGln-L-Lys is not subject to Edman degradation). In contrast, Edman degradation of *m/z* 2367.38 released five cycles of PT-Gly without releasing PT-Ala (Table 2). Thus, treatment of peptidoglycan with rLytN-generated fragments with either one (NH_2-Gly) or two (NH_2-Gly and NH_2-Ala) amino groups, in agreement with the proposed functions of LytN as MurNAc-L-Ala amidase and D-Ala-Gly endopeptidase.

TABLE 2
Edman degradation of rLytN released muropeptides

Cycle	Amino acid		
	m/z 724.68	*m/z* 796.69	*m/z* 2367.12
	pmol		
1	Ala (7.87); Gly (6.85)	Ala (5.39); Gly (6.69)	Gly (98.78)
2	Gly (10.88)	Gly (8.51)	Gly (91.47)
3	Gly (7.87)	Gly (6.56)	Gly (80.81)
4	Gly (6.10)	Gly (5.46)	Gly (72.95)
5	Gly (6.75)	Gly (3.72)	Gly (63.28)

Release of Cell Wall Anchored Protein A with Murein Hydrolases—Surface proteins of *S. aureus* and other Gram-positive bacteria are linked to peptidoglycan by a transpeptidation reaction (41). Sortase A cleaves the C-terminal sorting signal of surface proteins between the threonine and the glycine residues of the LP*X*TG motif (42) and forms an amide bond between the C-terminal threonine and the amino group of the pentaglycine cross-bridge (43). The cell wall anchor of surface proteins is embedded within peptidoglycan, *i.e.* anchor peptides are cross-linked to wall peptides of neighboring peptidoglycan strands, and the MurNAc-GlcNAc disaccharide of each anchor unit is located within long glycan chains (44, 45).

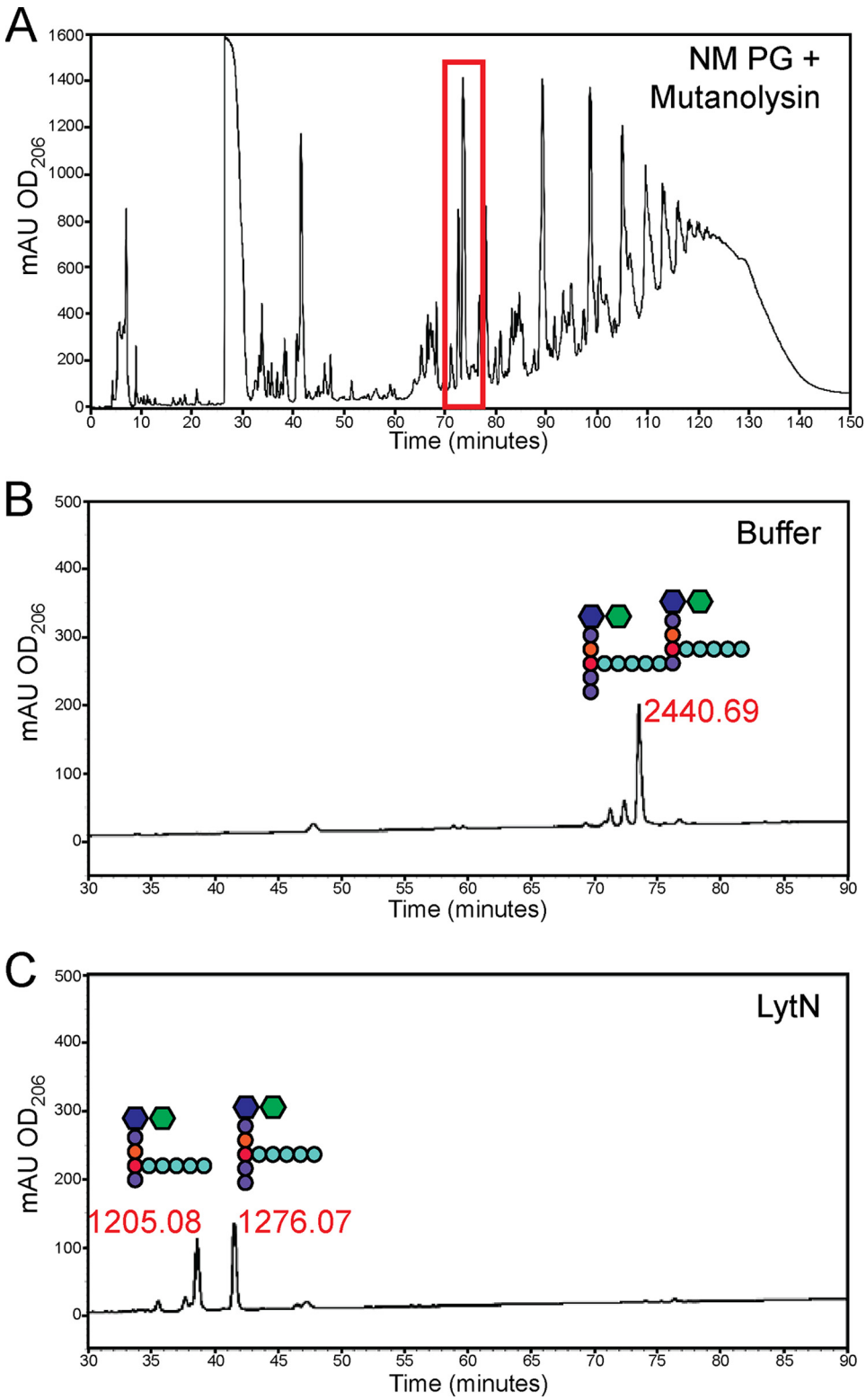

FIGURE 7. **rLytN-specific activity using muramidase-derived muropeptide substrates.** *A,* representative chromatograph of peptidoglycan from wild-type staphylococci treated with mutanolysin. The peak at 74 min (highlighted with a *red box*) represents a cross-linked peptidoglycan subunit. *B,* sample of peak 74 was split into two, and one half was treated with buffer alone and resolved again by rpHPLC. The peak was desalted and subjected to MALDI-TOF MS, with the mass listed above as well the structure of the muropeptide. *C,* sample of peak 74 was treated with rLytN for 4 h and examined as described in *B*. *mAU*, milliabsorbance units.

Treatment of peptidoglycan with muramidase (mutanolysin) solubilizes cell wall anchored protein A as a spectrum of fragments linked to C-terminal peptidoglycan with variable numbers of cross-linked subunits (Fig. 6, *C* and *D*) (45). Conversely, treatment of peptidoglycan with lysostaphin, a glycyl-glycine endopeptidase, solubilizes protein A with two to three C-termi-

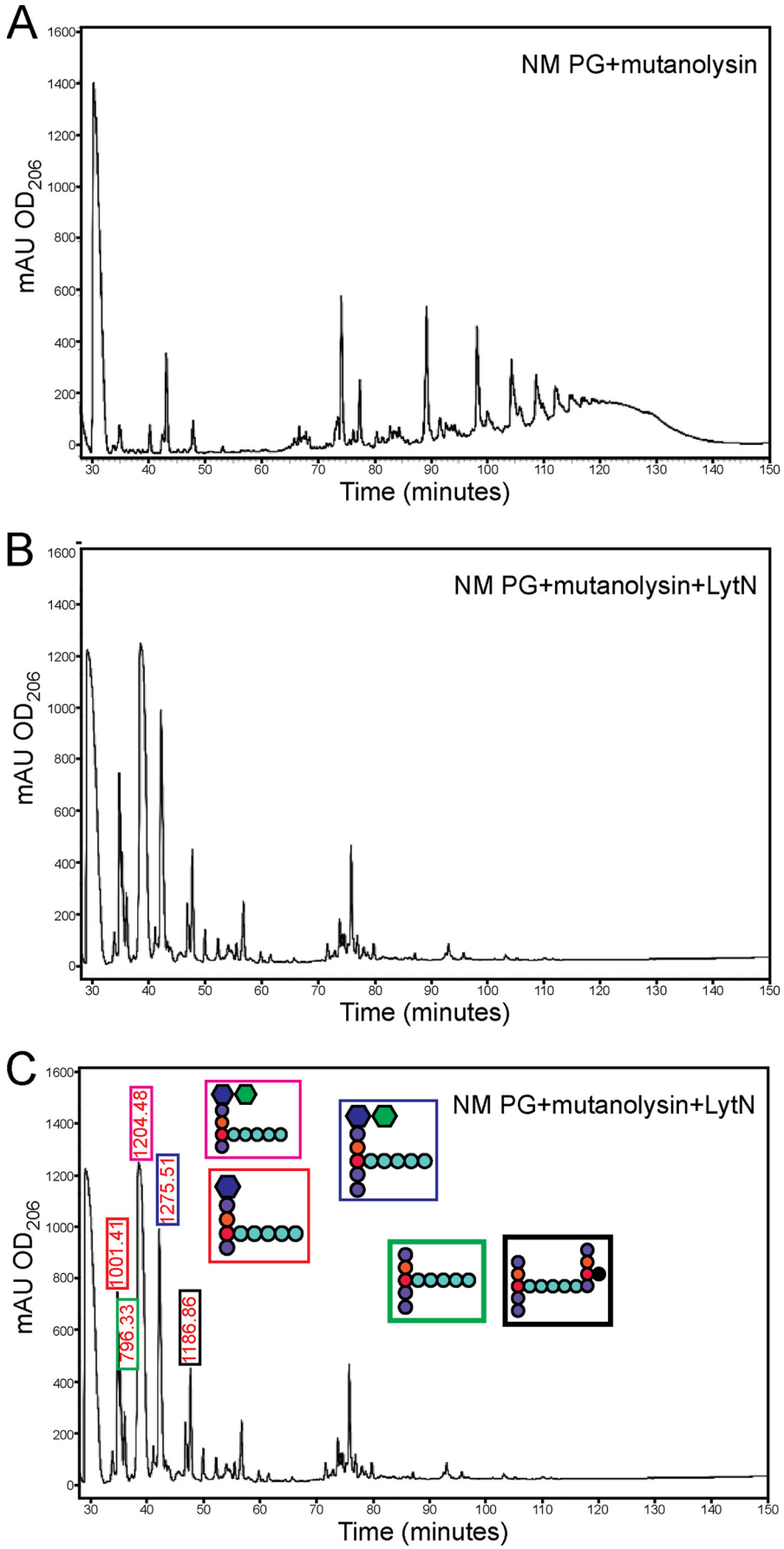
A
NM PG+mutanolysin
mAU OD206
Time (minutes)
B
NM PG+mutanolysin+LytN
mAU OD206
Time (minutes)
C
NM PG+mutanolysin+LytN
1204.48
1275.51
1001.41
796.33
1186.86
mAU OD206
Time (minutes)

TABLE 3
MALDI-TOF mass spectrometry of mutanolysin and rLytN treated peptidoglycan fragments

Compound	*m/z*		Δ (observed and calculated)	Predicted structure
	Observed	Calculated		
1	796.33	795.80	0.53	$AQKG_5AA$
2	1001.41	1001.01	0.40	$MurNAc\text{-}AQKG_5A$
3	1204.48	1205.20	−0.72	$GlcNAc\text{-}MurNAc\text{-}AQKG_5A$
4	1275.51	1275.24	0.27	$GlcNAc\text{-}MurNAc\text{-}AQKG_5AA$

nal glycine residues (average mass increase of 57–114 Da) (43). Lysostaphin-solubilized protein A migrates as a single species on SDS-PAGE, because the mass difference of one glycine residue (57 Da) cannot be resolved with this technology. Similar to lysostaphin, rLytN treatment solubilized protein A also as a single species on SDS-PAGE (Fig. 6*C*). rLytN-solubilized protein A migrated more slowly on SDS-PAGE than the lysostaphin-released counterpart (Fig. 6*C*). This can be explained by the MurNAc-L-Ala amidase and D-Ala-Gly endopeptidase activities of LytN, which released surface protein attached to a C-terminal anchor unit (NH_2-L-Ala-iGln-L-Lys-(NH_2-Gly_5)-D-Ala-COOH, 725 Da) (23).

Treatment of Cross-linked Murein Disaccharides with LytN—Purified peptidoglycan was treated with mutanolysin and subjected to rpHPLC. Cross-linked murein disaccharide MurNAc-(L-Ala-iGln-L-Lys-(NH_2-Gly_5)-D-Ala-Gly_5)-D-Ala-D-Ala-COOH)-(β1–4)-GlcNAc and MurNAc-(L-Ala-iGln-L-Lys-(NH_2-Gly_5)-D-Ala-COOH)-(β1–4)-GlcNAc was isolated, and mass was measured (*m/z* 2440.69). The sample was treated with rLytN, and cleavage products were resolved by rpHPLC and analyzed by MALDI-TOF mass spectrometry (Fig. 7). Two products were isolated, which generated ion signals with *m/z* 1205.08 and 1276.07. As a control, incubation with buffer alone did not affect the substrate at *m/z* 2440.69 (Fig. 7). These data indicated that rLytN cut *m/z* 2440.69 at the amide bond between D-Ala-Gly to generate MurNAc-(L-Ala-iGln-L-Lys-(Gly_5)-D-Ala-D-Ala-COOH)-(β1–4)-GlcNAc (*m/z* 1276.07) and MurNAc-(L-Ala-iGln-L-Lys-(NH_2-Gly_5)-D-Ala-COOH)-(β1–4)-GlcNAc (*m/z* 1205.08). Of note, MurNAc-L-Ala amidase activity was not observed when cross-linked murein disaccharides were incubated with rLytN. Similar results were observed when rLytN was incubated with other cross-linked disaccharides (supplemental Fig. S3). Even upon incubation of the monomeric peptidoglycan fragment, MurNAc-(L-Ala-iGln-L-Lys-(Gly_5)-D-Ala-D-Ala-COOH)-(β1-4)-GlcNAc, no rLytN cleavage products were observed (supplemental Fig. S3).

Treatment of Muramidase-digested Peptidoglycan with rLytN—We asked whether rLytN MurNAc-L-Ala amidase activity occurred not only with murein sacculi but also when muramidase-treated peptidoglycan was used as substrate. Purified peptidoglycan was first treated with mutanolysin. As a control, cleavage products were analyzed by rpHPLC. The sample was then split and either incubated with rLytN or left untreated. Reaction products were separated by rpHPLC (Fig. 8). rLytN treatment converted cross-linked peptidoglycan of mutanolysin digested murein to monomeric peptidoglycan. Most of the rLytN-generated peptidoglycan fragments represented disaccharide (MurNAc-GlcNAc) or monosaccharide (MurNAc) peptides that had been liberated by D-Ala-Gly endopeptidase cleavage (Fig. 8). For example, the most abundant ion, *m/z* 1204.48, represented MurNAc-(L-Ala-iGln-L-Lys-(NH_2-Gly_5)-D-Ala-COOH)-(β1–4)-GlcNAc. Nevertheless, we also observed *m/z* 796.44, a cleavage product with the structure NH_2-L-Ala-iGln-L-Lys-(NH_2-Gly_5)-D-Ala-D-Ala-COOH (calculated *m/z* 795.80). A complete listing of the observed ions and their proposed structure is presented in Table 3. As small amounts of wall peptide without disaccharide have been reported in muramidase-treated peptidoglycan samples, we presume that LytN cannot cleave the MurNAc-L-Ala amide bond of murein disaccharides. Nevertheless, rLytN is able to cleave this bond within fully assembled peptidoglycan.

Characterization of the CHAP Domain of LytN—The CHAP domains of other murein hydrolases have been shown to display single activities, either amidase or endopeptidase. Our results suggest that LytN may be able to perform both. We queried whether these functions may be performed by the CHAP domain or whether LytN harbored a second functional module. CHAP domains harbor conserved cysteine and histidine residues essential for activity (20, 21, 46). To determine the role of the CHAP domain of LytN, we generated a rLytN variant without the C-terminal CHAP domain (rLytNΔ_{CHAP}). Treatment of purified peptidoglycan with rLytNΔ_{CHAP} did not solubilize peptidoglycan fragments or degrade the murein sacculi. Similarly, variants with alanine substitutions at Cys^{266} (rLytN$_{C266A}$) or His^{329} (rLytN$_{H329A}$) did not display murein hydrolase activity (Fig. 9). To examine whether loss of function was caused by improper folding, rLytN and its variants were subjected to circular dichroism, which produced superimposable spectra in agreement with the hypothesis that the mutations do not affect folding and that Cys^{266} and His^{329} are required for catalysis (Fig. 9). Together, these data suggest that the conserved residues of the CHAP domain are necessary for rLytN activity and that the CHAP domain contributes to both the amidase and endopeptidase functions of LytN.

DISCUSSION

Homologs of LytN, a murein hydrolase whose YSIRK/GS signal peptide directs precursor secretion to the cross-wall of *S. aureus*, are found only in staphylococcal species. These bacteria

FIGURE 8. **Sequential digestion of peptidoglycan using muramidase and rLytN.** *A, S. aureus* wild-type peptidoglycan was treated with mutanolysin. *B,* wild-type peptidoglycan was first treated with mutanolysin, and the soluble muropeptides were then digested with rLytN and resolved by rpHPLC. *C,* muropeptides derived in *B* were desalted and subjected to MALDI-TOF MS. Shown *above* particular peaks are the *m/z* values of ions detected. *Color-coded boxes* demonstrate proposed structures for selected compounds. *mAU*, milliabsorbance units.

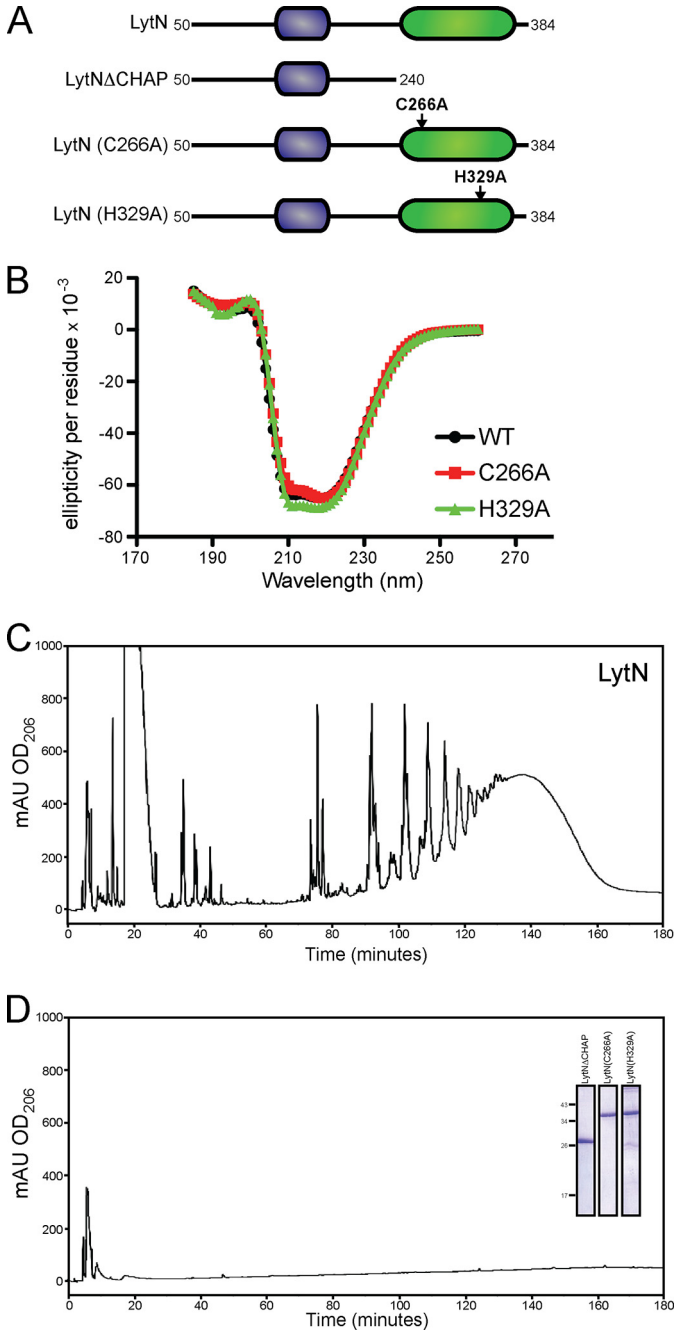

FIGURE 9. **CHAP domain of LytN is required for hydrolytic activity.** *A,* diagram of the primary structure of rLytN constructs in which the CHAP domain is removed or specific amino acid substitutions have been introduced. Mutated amino acids are indicated with *arrows*. *B,* circular dichroism spectra of rLytN or its C266A and H329A substitution variants were analyzed in the far-UV range. *C,* rpHPLC of soluble rLytN-treated muropeptides. *D,* rpHPLC of muropeptides generated upon incubation of peptidoglycan with $rLytN_{\Delta CHAP}$. The C266A and H329A variants also failed to cleave staphylococcal peptidoglycan. *Inset,* Coomassie Brilliant Blue-stained SDS-PAGE samples of purified $rLytN_{\Delta CHAP}$, $rLytN_{C266A}$, and $rLytN_{H329A}$. *mAU*, milliabsorbance units.

replicate by a distinctive program, whereby cell division planes are built perpendicular to previous planes (13) and bulk *de novo* peptidoglycan synthesis occurs at the cross-wall, the peptidoglycan layer that separates a mother cell into two daughters (47). *S. aureus* mutants lacking *lytN* display delayed growth as well as structural defects to the cell wall envelope in that the otherwise homogeneous appearance of peptidoglycan is perturbed, giving rise to disordered layers of cell wall and irregular cell shapes. Synthesis and secretion of LytN must be carefully controlled, as increased expression of *lytN* triggered the rupture of cross-walls as well as lysis of staphylococci. Although overexpressed LytN could be detected by immunoblot, this technology did not reveal the overall abundance or the stability of the murein hydrolase under physiological conditions. Of note, intracellular LytN precursor with its YSIRK/GS signal peptide, but not extracellular purified rLytN, can fully complement the growth phenotype of *lytN* mutants. Future research must resolve whether synthesis, secretion, and degradation of LytN occur constitutively or in a regulated manner, accompanying discrete steps in staphylococcal cytokinesis.

LytN harbors a CHAP domain. Similar domains have been found in murein hydrolases from several different Gram-positive bacteria (21). Although conserved throughout bacteria and even eukaryotes, the function of this domain is not definitively known. Examples exist within parasitic species whereby the CHAP domain is not at all related to peptidoglycan metabolism (19). Where tested, bacterial enzymes with CHAP domains have been reported to cleave peptidoglycan either as a MurNAc-L-Ala amidase (18) or a D-Ala-Gly endopeptidase (23). To the best of our knowledge, we report here for the first time that LytN, an enzyme with a CHAP domain, can exert both activities. The evidence for this is as follows. Treatment of purified staphylococcal peptidoglycan with rLytN released uncross-linked wall peptides (L-Ala-D-iGln-L-Lys(NH_2-Gly_5)-D-Ala) both with and without linked disaccharide (MurNAc-GlcNAc). Additionally, rLytN treatment of staphylococcal cells liberated protein A attached to a single peptidoglycan fragment, not a spectrum of cross-linked fragments. This result can only be explained as the release of surface protein anchor structures from both the glycan strands (MurNAc-L-Ala amidase activity) and the cross-linked peptidoglycan (D-Ala-Gly endopeptidase activity) of the staphylococcal cell wall (48). Curiously, pretreatment of peptidoglycan with muramidase (mutanolysin) did not permit detection of LytN amidase activity without impacting the endopeptidase activity of the enzyme. One plausable explanation for these data is that LytN amidase requires either intact glycan strands or MurNAc reducing ends, a product of glucosaminidase cleavage. GlcNAc reducing ends, generated via muramidase treatment of peptidoglycan, apparently do not support LytN amidase activity. The genome of *S. aureus* encodes for several murein hydrolases with glucosaminidase or CHAP domains but not for muramidases (22). We wonder whether the observed glycan substrate requirements for dual enzyme activity represent a general feature of murein hydrolases with CHAP domains. For *S. aureus*, this attribute could apply to Sle1 (18), LytA, ϕ11 hydrolase (23), and LytN.

Two staphylococcal murein hydrolases harbor LysM domains, Sle1 (23) and LytN. A third protein, Atl, harbors three repeat domains that are similar in size but lack sequence similarity with LysM domains (49). All three proteins are directly involved in cleaving the cross-wall and enabling daughter cell separation following the completion of staphylococcal cytokinesis (5). Two secreted proteins, Atl and Sle1, accomplish this task by associating with the bacterial peptidoglycan. For Atl, this involves binding to the envelope in the vicinity of the cross-

wall or cell division site (14, 49). We presume, but do not know, that Sle1 may also target to this site (18). In contrast to Atl and Sle1, LytN harbors a single LysM domain (22). When added exogenously to staphylococci, rLytN binds to the cell wall envelope. Unlike Atl (15), however, rLytN appears to be distributed all over the envelope, *i.e.* it is not restricted to the cell division site. Nevertheless, murein hydrolases with LysM domains appear specifically involved in the separation of cell wall during cytokinesis (50). For secreted proteins, this involves multiple LysM domains (50–53), whereas LytN harbors only one of these domains. Thus, identification of the cell wall ligand for the LysM domain may provide important insights into the physiology of bacterial cell wall separation and cytokinesis. We hypothesize that the LysM domain, rather than conferring substrate specificity as has been postulated for Sle1, provides LytN, which has been delivered to the cross-wall via its YSIRK signal peptide, peptidoglycan binding, and envelope association of this enzyme. In conclusion, we propose a revised model for staphylococcal separation following cytokinesis, whereby Atl and Sle1 are initially secreted into the extracellular milieu and bind the cell wall envelope in the vicinity of the cross-wall. Atl and Sle1 then split the cross-wall from the outside in. In contrast, LytN is secreted directly into the cross-wall and splits the cross-wall from the inside out, thereby separating staphylococcal daughter cells.

Acknowledgments—We thank Justin Kern and Stefan Richter for expert assistance with the HPLC and mass spectrometry analysis. We also thank Valerie Anderson for helpful discussions and experimental assistance and all members of the laboratory for critical comments on the manuscript.

REFERENCES

1. Lowy, F. D. (1998) *N. Engl. J. Med.* **339,** 520–532
2. Klevens, R. M., Edwards, J. R., Gaynes, R. P., and National Nosocomial Infections Surveillance System (2008) *Clin. Infect. Dis.* **47,** 927–930
3. Hiramatsu, K., Hanaki, H., Ino, T., Yabuta, K., Oguri, T., and Tenover, F. C. (1997) *J. Antimicrob. Chemother.* **40,** 135–136
4. Chang, S., Sievert, D. M., Hageman, J. C., Boulton, M. L., Tenover, F. C., Downes, F. P., Shah, S., Rudrik, J. T., Pupp, G. R., Brown, W. J., Cardo, D., and Fridkin, S. K. (2003) *N. Engl. J. Med.* **348,** 1342–1347
5. Giesbrecht, P., Kersten, T., Maidhof, H., and Wecke, J. (1998) *Microbiol. Mol. Biol. Rev.* **62,** 1371–1414
6. Chatterjee, A. N., and Park, J. T. (1964) *Proc. Natl. Acad. Sci. U.S.A.* **51,** 9–16
7. Berger-Bächi, B. (1994) *Trends Microbiol.* **2,** 389–393
8. Strominger, J. L., Izaki, K., Matsuhashi, M., and Tipper, D. J. (1967) *Fed. Proc.* **26,** 9–22
9. Tipper, D. J., and Strominger, J. L. (1965) *Proc. Natl. Acad. Sci. U.S.A.* **54,** 1133–1141
10. Tipper, D. J., and Strominger, J. L. (1968) *J. Biol. Chem.* **243,** 3169–3179
11. Ghuysen, J. M. (1968) *Bacteriol. Rev.* **32,** 425–464
12. Navarre, W. W., and Schneewind, O. (1999) *Microbiol. Mol. Biol. Rev.* **63,** 174–229
13. Tzagoloff, H., and Novick, R. (1977) *J. Bacteriol.* **129,** 343–350
14. Yamada, S., Sugai, M., Komatsuzawa, H., Nakashima, S., Oshida, T., Matsumoto, A., and Suginaka, H. (1996) *J. Bacteriol.* **178,** 1565–1571
15. Komatsuzawa, H., Sugai, M., Nakashima, S., Yamada, S., Matsumoto, A., Oshida, T., and Suginaka, H. (1997) *Microbiol. Immunol.* **41,** 469–479
16. Oshida, T., Sugai, M., Komatsuzawa, H., Hong, Y. M., Suginaka, H., and Tomasz, A. (1995) *Proc. Natl. Acad. Sci. U.S.A.* **92,** 285–289
17. Sugai, M., Yamada, S., Nakashima, S., Komatsuzawa, H., Matsumoto, A., Oshida, T., and Suginaka, H. (1997) *J. Bacteriol.* **179,** 2958–2962
18. Kajimura, J., Fujiwara, T., Yamada, S., Suzawa, Y., Nishida, T., Oyamada, Y., Hayashi, I., Yamagishi, J., Komatsuzawa, H., and Sugai, M. (2005) *Mol. Microbiol.* **58,** 1087–1101
19. Baba, T., and Schneewind, O. (1998) *Trends Microbiol.* **6,** 66–71
20. Rigden, D. J., Jedrzejas, M. J., and Galperin, M. Y. (2003) *Trends Biochem. Sci.* **28,** 230–234
21. Bateman, A., and Rawlings, N. D. (2003) *Trends Biochem. Sci.* **28,** 234–237
22. Baba, T., Bae, T., Schneewind, O., Takeuchi, F., and Hiramatsu, K. (2008) *J. Bacteriol.* **190,** 300–310
23. Navarre, W. W., Ton-That, H., Faull, K. F., and Schneewind, O. (1999) *J. Biol. Chem.* **274,** 15847–15856
24. DeDent, A., Bae, T., Missiakas, D. M., and Schneewind, O. (2008) *EMBO J.* **27,** 2656–2668
25. Bae, T., and Schneewind, O. (2003) *J. Bacteriol.* **185,** 2910–2919
26. Mazmanian, S. K., Ton-That, H., Su, K., and Schneewind, O. (2002) *Proc. Natl. Acad. Sci. U.S.A.* **99,** 2293–2298
27. Sugai, M., Fujiwara, T., Komatsuzawa, H., and Suginaka, H. (1998) *Gene* **224,** 67–75
28. Berger-Bächi, B., Barberis-Maino, L., Strässle, A., and Kayser, F. H. (1989) *Mol. Gen. Genet.* **219,** 263–269
29. Bae, T., Banger, A. K., Wallace, A., Glass, E. M., Aslund, F., Schneewind, O., and Missiakas, D. M. (2004) *Proc. Natl. Acad. Sci. U.S.A.* **101,** 12312–12317
30. Bae, T., Baba, T., Hiramatsu, K., and Schneewind, O. (2006) *Mol. Microbiol.* **62,** 1035–1047
31. Kreiswirth, B. N., Löfdahl, S., Betley, M. J., O'Reilly, M., Schlievert, P. M., Bergdoll, M. S., and Novick, R. P. (1983) *Nature* **305,** 709–712
32. Frankel, M. B., Wojcik, B. M., DeDent, A. C., Missiakas, D. M., and Schneewind, O. (2010) *Mol. Microbiol.* **78,** 238–252
33. Lee, C. Y., Buranen, S. L., and Ye, Z. H. (1991) *Gene* **103,** 101–105
34. Gründling, A., and Schneewind, O. (2007) *Proc. Natl. Acad. Sci. U.S.A.* **104,** 8478–8483
35. de Jonge, B. L., Chang, Y. S., Gage, D., and Tomasz, A. (1992) *J. Biol. Chem.* **267,** 11248–11254
36. Glauner, B., Höltje, J. V., and Schwarz, U. (1988) *J. Biol. Chem.* **263,** 10088–10095
37. DeDent, A. C., McAdow, M., and Schneewind, O. (2007) *J. Bacteriol.* **189,** 4473–4484
38. Cheng, A. G., Kim, H. K., Burts, M. L., Krausz, T., Schneewind, O., and Missiakas, D. M. (2009) *FASEB J.* **23,** 3393–3404
39. Schindler, C. A., and Schuhardt, V. T. (1964) *Proc. Natl. Acad. Sci. U.S.A.* **51,** 414–421
40. Yokogawa, K., Kawata, S., Nishimura, S., Ikeda, Y., and Yoshimura, Y. (1974) *Antimicrob. Agents Chemother.* **6,** 156–165
41. Mazmanian, S. K., Liu, G., Ton-That, H., and Schneewind, O. (1999) *Science* **285,** 760–763
42. Navarre, W. W., and Schneewind, O. (1994) *Mol. Microbiol.* **14,** 115–121
43. Schneewind, O., Fowler, A., and Faull, K. F. (1995) *Science* **268,** 103–106
44. Ton-That, H., Faull, K. F., and Schneewind, O. (1997) *J. Biol. Chem.* **272,** 22285–22292
45. Navarre, W. W., Ton-That, H., Faull, K. F., and Schneewind, O. (1998) *J. Biol. Chem.* **273,** 29135–29142
46. Donovan, D. M., Foster-Frey, J., Dong, S., Rousseau, G. M., Moineau, S., and Pritchard, D. G. (2006) *Appl. Environ. Microbiol.* **72,** 5108–5112
47. Giesbrecht, P., Wecke, J., and Reinicke, B. (1976) *Int. Rev. Cytol.* **44,** 225–318
48. Marraffini, L. A., Dedent, A. C., and Schneewind, O. (2006) *Microbiol. Mol. Biol. Rev.* **70,** 192–221
49. Baba, T., and Schneewind, O. (1998) *EMBO J.* **17,** 4639–4646
50. Mesnage, S., Chau, F., Dubost, L., and Arthur, M. (2008) *J. Biol. Chem.* **283,** 19845–19853
51. Buist, G., Kok, J., Leenhouts, K. J., Dabrowska, M., Venema, G., and Haandrikman, A. J. (1995) *J. Bacteriol.* **177,** 1554–1563
52. Carroll, S. A., Hain, T., Technow, U., Darji, A., Pashalidis, P., Joseph, S. W., and Chakraborty, T. (2003) *J. Bacteriol.* **185,** 6801–6808
53. Steen, A., Buist, G., Horsburgh, G. J., Venema, G., Kuipers, O. P., Foster, S. J., and Kok, J. (2005) *FEBS J.* **272,** 2854–2868